

High Resolution ISAR Imaging Based on Improved Smoothed l_0 Norm Recovery Algorithm

Junjie Feng^{1,2} and Gong Zhang^{1,2}

¹ Key Laboratory of Radar Imaging and Microwave Photonics, Ministry of Education,
Nanjing, 210016, China
[e-mail: fzy028@163.com]

² College of Electronic and Information Engineering, Nanjing University of Aeronautics and Astronautics,
Nanjing, 210016, China

[e-mail: gongzhang_nuaa@163.com]

*Corresponding author: Junjie Feng

*Received September 2, 2015; revised October 21, 2015; accepted October 28, 2015;
published December 31, 2015*

Abstract

In radar imaging, a target is usually consisted of a few strong scatterers which are sparsely distributed. In this paper, an improved sparse signal recovery algorithm based on smoothed l_0 (SLO) norm method is proposed to achieve high resolution ISAR imaging with limited pulse numbers. Firstly, one new smoothed function is proposed to approximate the l_0 norm to measure the sparsity. Then a single loop step is used instead of two loop layers in SLO method which increases the searching density of variable parameter to ensure the recovery accuracy without increasing computation amount, the cost function is undated in every loop for the next loop until the termination is satisfied. Finally, the new set of solution is projected into the feasible set. Simulation results show that the proposed algorithm is superior to the several popular methods both in terms of the reconstruction performance and computation time. Real data ISAR imaging obtained by the proposed algorithm is competitive to several other methods.

Keywords: High resolution imaging, inverse synthetic aperture radar (ISAR), sparse signal recovery, smoothed l_0 norm

This work was supported by the Chinese National Natural Science Foundation under contract No. 61201367, 61271327, 61471191, and partly funded by the Priority Academic Program Development of Jiangsu Higher Education Institutions (PADA).

1. Introduction

Inverse synthetic aperture radar (ISAR) imaging has received much attention in the past three decades [1]-[3]. ISAR imaging is widely used in many military and civilian applications, such as target identification and aircraft traffic control. In the conventional ISAR imaging, the observing interval must be long enough so that a high cross-range resolution can be obtained by a coherent integration. To obtain high resolution, ISAR imaging always needs many measurements in range frequency and cross-range time domains. For a long coherent processing interval, the target may move with maneuvering. If the rotation angle is too large, the Radar Cross Section (RCS) of the scatterer may be time varying which increases the difficulty of coherent processing. So implementing imaging in a short time duration is meaningful.

In recent years, compressive sensing (CS) has become very popular in signal processing [4]-[9]. CS provides a new sampling paradigm which is able to reconstruct the sparse or compressible signals exactly from limited measurements by solving an optimization problem. It is a technique proposed to improve signal separation ability using a prior sparse property information of the signal. Sparsity usually can be measured by l_p ($0 \leq p \leq 1$) norm [10]. The sparse signal recovery is a key step in CS. Although l_0 norm is better in describing sparsity of noise free case, sparse signal recovery algorithms based on l_0 norm are intractable because they are sensitive to noise and need combinatorial search. The reconstruction algorithms based on l_1 norm are computationally complex, which limits their practical applications. Hence many simpler algorithms, such as orthogonal matching pursuit (OMP) [11][12] are proposed. However, they are iteratively greedy algorithms and do not give good estimation of the sources.

Mohimani et al proposed a smoothed function to approximate l_0 norm, then the problem of minimum l_0 norm optimization can be transferred to an optimization problem of smoothed functions. The method called smoothed l_0 norm (SLO) method [13]. The SLO method is about two orders of magnitude faster than l_1 -magic method, while providing better estimation of the source than l_1 -magic method.

For radar imaging, a target is usually regarded as consist of a few strong scatterers and the distribution of these strong scatterers is sparse in the imaging volume. Then sparse learning methods can be used to improve radar imaging quality [14]-[17], such as SAR/ISAR imaging [18][19], MIMO radar imaging [20][21], and so on.

For ISAR imaging, this has been shown that combining ISAR and sparse learning can improve the 2D image quality with limited measured data [22]. Combination of local sparsity constraint and nonlocal total variation are discussed in [23]. The application of CS to ISAR imaging of moving targets in sea clutter is discussed in [24]. A multi-task Bayesian model is utilized for ISAR in [25]. Fully polarimetric ISAR imaging based on CS is discussed in [26].

In this paper, we proposed a new reconstruction algorithm based on SLO method to improve ISAR imaging quality. One new continuous sequence is proposed as smoothed function to approach the l_0 norm which is suit to measure sparsity. Then one single loop step is used to replace two loop layers in SLO algorithm which increase the searching density of variable

parameters. The proposed algorithm ensures the reconstruction accuracy and the computation amounts don't increase. By using the improved algorithm, ISAR imaging is more intensive with limited pulse numbers. Real data ISAR images obtained using the proposed method is competitive to the several popular methods.

This paper is organized as follows. Section 2 introduces necessary ISAR model and sparse learning imaging formation. In section 3, the proposed reconstruction algorithm is introduced in detail. Simulation and real data ISAR imaging results are presented in section 4. Finally, section 5 provides the conclusion and discussion.

2. ISAR Imaging Model Based On Sparse Learning

In order to facilitate analysis, it can be assumed that the translational motion of the target has been completely compensated via conventional methods. During the coherent processing interval (CPI), the radar transmits linear frequency modulation modulated signal can be defined as

$$s(\tau) = \text{rect}\left(\frac{\hat{t}}{T_p}\right) \exp\left[j2\pi\left(f_c \hat{t} + \frac{1}{2} \gamma \hat{t}^2\right)\right] \quad (1)$$

where $\hat{t} = t \bmod(\Delta t)$ is the fast time, t is the slow time, Δt is the pulse repetition duration, f_c is the carrier frequency, γ is the chirp rate, T_p is the pulse width, $\text{rect}(\cdot)$ is the rectangle pulse function. Then the complex echo signal is

$$s(\hat{t}, t) = A \cdot \text{rect}\left(\frac{\hat{t}}{T_p}\right) \cdot \text{rect}\left(\frac{t}{T_a}\right) \cdot \exp\left\{j2\pi\left[\left(\hat{t} - \frac{2R(t)}{c}\right) + \frac{1}{2} \gamma \left(\hat{t} - \frac{2R(t)}{c}\right)^2\right]\right\} \quad (2)$$

where c is the light speed, T_a is the CPI, A is the backward scattering amplitude which can be viewed stationary during the CPI. After the range compression, the received signal can be described as

$$s(\hat{t}, t) = A \cdot \text{rect}\left(\frac{\hat{t}}{T_a}\right) \cdot \text{sinc}\left[T_p \left(\hat{t} - \frac{2R(t)}{c}\right)\right] \cdot \exp\left(-j4\pi \frac{R(t)}{\lambda}\right) \quad (3)$$

where λ is the wavelength. At different dwell time t , the received signal has different time delay in the fast time \hat{t} . After pulse compression by matched filtering and omitting the constant introduced, the received signal becomes

$$s(\hat{t}, t) = A \cdot \text{sinc}\left[T_p \gamma \left(\hat{t} - \frac{2(R_0 + y)}{c}\right)\right] \cdot \exp\left[-j4\pi \frac{(R_0 + y)}{\lambda}\right] \cdot \text{rect}\left(\frac{t}{T_a}\right) \cdot \exp\left[-j2\pi\left(f \cdot t + \frac{1}{2} \beta \cdot t^2\right)\right] \quad (4)$$

where $f = 2x\omega / \lambda$, $\beta = 2x\alpha / \lambda$ are the Doppler and Doppler rate respectively. Assuming a distance unit includes K scatterer points, the signal in the range cell corresponding to $\tau = 2(R_0 + y) / c$ by omitting the constant phase term can be written as

$$s(t) = \sum_{k=1}^K A_k \cdot \text{rect}\left(\frac{t}{T}\right) \cdot \exp(-j2\pi f_k t) + n \quad (5)$$

where A_k and f_k are the k th scattering centers' reflecting amplitude and Doppler frequency, respectively. n is the additive noise. The time sequence is $t = [1 : N]^T \cdot \Delta t$, $\Delta t = 1 / f_r$, being the time interval, f_k is the pulse repetition frequency. $N = T / \Delta t$ is the number of pulses. Δf_d is the Doppler frequency resolution, the sparse Doppler sequence is $f_d = [1 : Q] \cdot \Delta f_d$, $Q = f_r / \Delta f_d$, Q is the number of Doppler unit corresponding to Δf_d . Thus, the basis matrix can be constructed as $\Psi = \{\varphi_1, \varphi_2, \dots, \varphi_q, \dots, \varphi_Q\}$, $\varphi_q(t) = \exp(-j2\pi f_d(q)t)$, $0 \leq q \leq Q$.

Then the received discrete signal equation can be rewritten as

$$s = \Psi \theta + n \quad (6)$$

The nonzero components of θ in the sparse vector correspond to the amplitudes of the strong scatterers which are located in the grids. For compressive sensing, the optimization algorithms have been applied for real number. Equation (6) should be transformed into real number case. We divide the signal into the real and imaginary components as follows

$$\begin{aligned} y &= \begin{bmatrix} \Re(s) \\ \Im(s) \end{bmatrix}, & A &= \begin{bmatrix} \Re(\Psi) & -\Im(\Psi) \\ \Im(\Psi) & \Re(\Psi) \end{bmatrix} \\ \eta &= \begin{bmatrix} \Re(\theta) \\ \Im(\theta) \end{bmatrix}, & z &= \begin{bmatrix} \Re(n) \\ \Im(n) \end{bmatrix} \end{aligned} \quad (7)$$

where $\Re(\cdot)$ and $\Im(\cdot)$ express the real and imaginary part of the complex vector respectively. So the equation (6) becomes

$$y = A\eta + z \quad (8)$$

To solve η , we can use the following sparse optimization strategy

$$\hat{\eta} = \arg \min \|\eta\|_p \quad \text{s.t.} \quad \|y - A\eta\|_2 < \varepsilon, \quad (9)$$

where ε is a small positive number associated with z . p indicates the l_p norm. The imaging quality largely depends on reconstruction algorithms, an improved SL0 algorithm is proposed and applied to ISAR imaging. We give a detailed description about the algorithm in the

3. The Improve SL0 Imaging Algorithm

To obtain an approximate l_0 norm solution, a smoothed function $G_\sigma(\eta) = \sum_i \exp(-\frac{\eta_i^2}{2\sigma^2})$

was used to replace the l_0 norm in [13]. When a parameter σ approaches zero, the function $G_\sigma(\eta)$ approaches l_0 norm. A two-layer method was proposed to solve the sparse signal recovery problem. In order to improve the approximation performance of the smoothed function, we propose a continuous sequence as follow

$$f_{\sigma,\zeta}(\eta) = e^{-\frac{\sqrt{\eta^2+\zeta}}{\sigma}} \quad (10)$$

where σ is the variable parameter, ζ is a small positive element which ensures the function is continuous and differentiable. It is obvious that

$$\lim_{\sigma \rightarrow 0} f_{\sigma,\zeta}(\eta) = \begin{cases} 0, & \eta \neq 0 \\ 1, & \eta = 0 \end{cases} \quad (11)$$

Then denote

$$F_{\sigma,\zeta}(\eta) = \sum_{i=1}^N f_{\sigma,\zeta}(\eta_i) \quad (12)$$

where $\|\eta\|_0$ expresses the number of nonzero elements of vector η . According to the definition of l_0 norm, we can obtain $\|\eta\|_0 = \lim_{\sigma \rightarrow 0} F_{\sigma,\zeta}(\eta)$.

A property of $G_\sigma(\eta)$ is that when $\sigma \rightarrow \infty$, $N - G_\sigma(\eta)$ approaches l_2 norm. However, for $F_{\sigma,\zeta}(\eta)$, when $\sigma \rightarrow \infty$, $N - F_{\sigma,\zeta}(\eta)$ approaches l_1 norm. When σ approximates zero, it approaches l_0 norm. For l_1 norm can describe sparsity, we can search for the sparse solution with high probability at the beginning of iteration.

Therefore sparse signal recovery algorithm based on function $F_{\sigma,\zeta}(\eta)$ minimum can be described as

$$\hat{\eta} = \lim_{\sigma \rightarrow \sigma_{\min}} \operatorname{argmin} F_{\sigma,\zeta}(\eta) \quad s.t. \|y - A\eta\|_2 < \varepsilon \quad (13)$$

In the proposed algorithm, we use one loop layer to replace two loop layers in SL0 algorithm. For smoothed l_0 norm algorithm presented in [13], two layer loop is used to obtain the minimum solution. Generally speaking, if the inner iterative number is large enough, the step size can be small. Actually, obtaining a precise solution in inner loop is not necessary. The aim of inner loop is to provide an initial value for the outer loop. Since the double loop does not need to find out the real point, we use single layer to replace two loop layers and increase the searching density of variable parameter σ at the same time which search a point approaches to the minimum solution in each iteration. The proposed algorithm called ISSLO. We add a step which compare the old cost function and new cost function. If Newfunction is greater than Oldfunction, the loop stops, otherwise, continues to the next loop. When the parameter σ approaches zero, F_σ approaches l_0 norm. If New function is greater than Old function, the solution is the minimum point at this time. Then the loop stops which can save the computation amount. The ISSLO algorithm ensures the reconstruction accuracy and the computation amount don't increase compared with SL0 algorithm. The gradient projection method is used to project new iteration position to the feasible set. The total ISSLO optimization algorithm in this paper can be summarized as follows:

Initialization:

1) Let $\hat{\eta}_0$ be equal to the minimum l_2 norm solution of $y = A\eta$, obtained by

$$\hat{\eta}_0 = A^H(AA^H)^{-1}y.$$

2) Choose a suitable decreasing sequence for $\{\sigma\}, [\sigma_1, \dots, \sigma_J]$.

for $j = 1, \dots, J$

- (1) Let $\sigma = \sigma_j$, $\beta = \frac{J-j+1}{J}$
 Oldfunction = $N - \text{sum}(F_{\sigma,\zeta}(\eta))$.
- (2) Minimize the function $F_{\sigma,\zeta}(\eta)$ on the feasible set $\eta = \{\eta : \|A\eta - y\|_2 < \varepsilon\}$
- a) Initialization: $\eta = \hat{\eta}_{j-1}$
 - b) Let δ be gradient of $F_{\sigma,\zeta}(\eta)$.
 - c) For every element of η , let $\eta(n) \leftarrow \eta(n) - \mu\sigma\delta(n)$ (where μ is a small positive constant)
 - d) If $\|A\eta - y\|_2 > \varepsilon$, project η back into the feasible set η :

$$\eta \leftarrow \eta - A^H(AA^H)^{-1}(\eta - A\eta)$$
 - e) update $F_{\sigma,\zeta}(\eta)$.
- 3) Set $\hat{\eta}_j = \eta$.
- 4) Newfunction = $N - \text{sum}(F_{\sigma,\zeta}(\eta))$
 If Newfunction > Oldfunction
 break
 end

Final answer is $\hat{\eta} = \hat{\eta}_j$.

In the above algorithm, some initial parameters should be chosen. $\hat{\eta}_0 = A^H(AA^H)^{-1}y$ is the minimum l_2 norm solution. In [13], σ_1 is chosen as $\sigma_1 > 4 \max_i |\hat{\eta}_0(i)|$. In this paper, σ_1 should be chosen as $\sigma_1 > 16 \max_i |\hat{\eta}_0(i)|$. For l_0 norm is not suited to express a vector with many small elements, the choice of σ_j should not be too small. σ_j can be estimated by selecting a few noise samples, selecting the maximum value of $|A^H(AA^H)^{-1}z|$ and taking the average value. We choose σ_j as $\sigma_j = E(\max(|A^H(AA^H)^{-1}z|))$. For the choice of step size factor μ , at the beginning of search, we select a larger step size, when the searching point approaches the minimum solution, the step size should decrease. So in our algorithm, we choose step size as $\mu = \beta \max|\eta|/10$, with the increase of j (loop number), the adjust factor β decreases, then the step size decreases. $\max|\eta|$ term adjusts the step size to match the solution. The size of η is $M \times N$. The computational loads of the proposed algorithm are consisted of the step (c) to (d) in step 2) of each iteration. $A\eta$ needs MN multiplications in each iteration. So the computational complexity of the proposed method is $O(MN)$.

4. Experimental Results

Simulation 1. One Dimensional Synthetic Signals Recovery

The signal model with noise is $y = A\eta + z$, the size of $A (M \times N)$ is 128×256 , it is constructed by selecting its components from $N(0, 1)$. η is the sparse signal, whose nonzero coefficients are uniform ± 1 random spikes signal. We consider SNR=15, 20,25,30dB conditions. For SL_0 method, the numbers of outer loop and inner loop are 20 and 10 respectively. For ISSLO algorithm, the loop number is 200. The parameter $\zeta = 0.01$. The

MSE is defined as $\frac{1}{N} \|\eta - \hat{\eta}\|^2$, where η is the true solution and $\hat{\eta}$ is the estimation value.

The experiment was implemented 100 times (with the same parameters, but for different randomly generated sources and coefficient matrices). The computation time, reconstruction probability and MSE are averaged. **Fig. 1** shows the average computational time for 15dB SNR case. For other SNR cases, the computational time is similar to this case. From **Fig. 1**, we can see the computation costs of OMP, SL_0 and ISSLO are less than Bayesian and l1-ls methods. The reconstruction probability and MSE of different methods with different K are shown in **Fig. 2** and **Fig. 3**. The reconstruction probability of different methods decreases gradually with K increases. MSE of different methods increases gradually with K increases. We can see that with the increase of SNR, the performance of l1-ls and ISSLO methods improve faster than OMP, SL_0 and Bayesian methods. The performances of ISSLO algorithm are competitive with other algorithms especially when SNR is high and K is large.

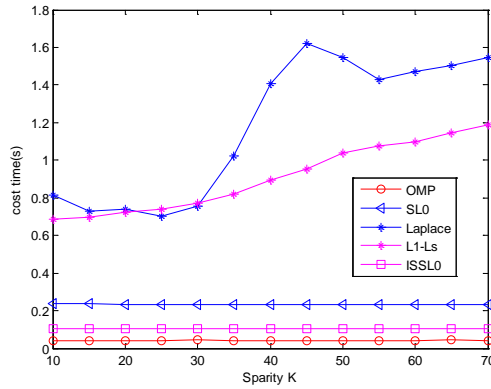
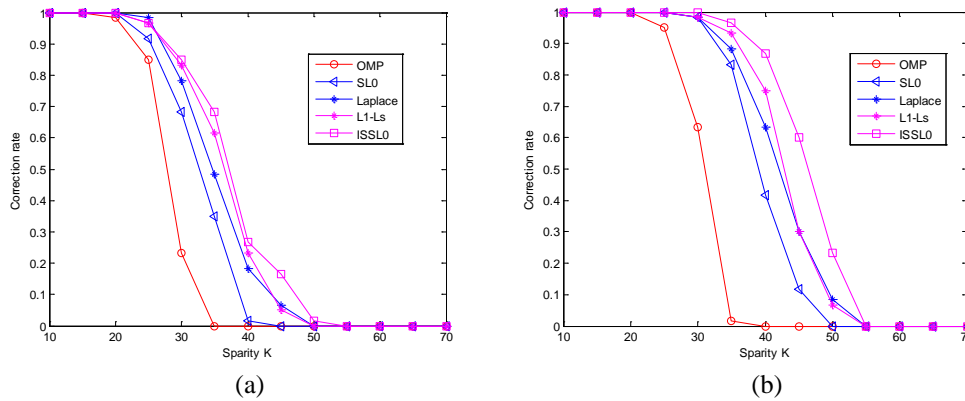


Fig. 1. Computation costs of different methods



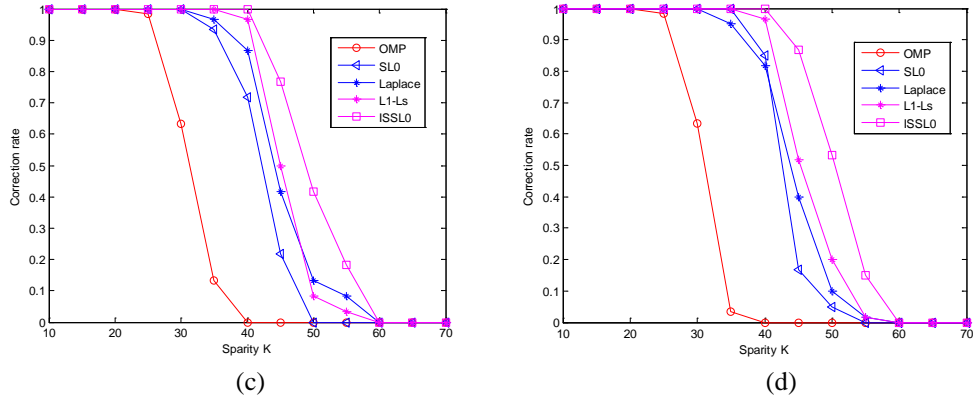


Fig. 2. Correct position estimation for different K (a) SNR=15dB (b)SNR=20dB (c) SNR =25dB, (d) SNR = 30dB

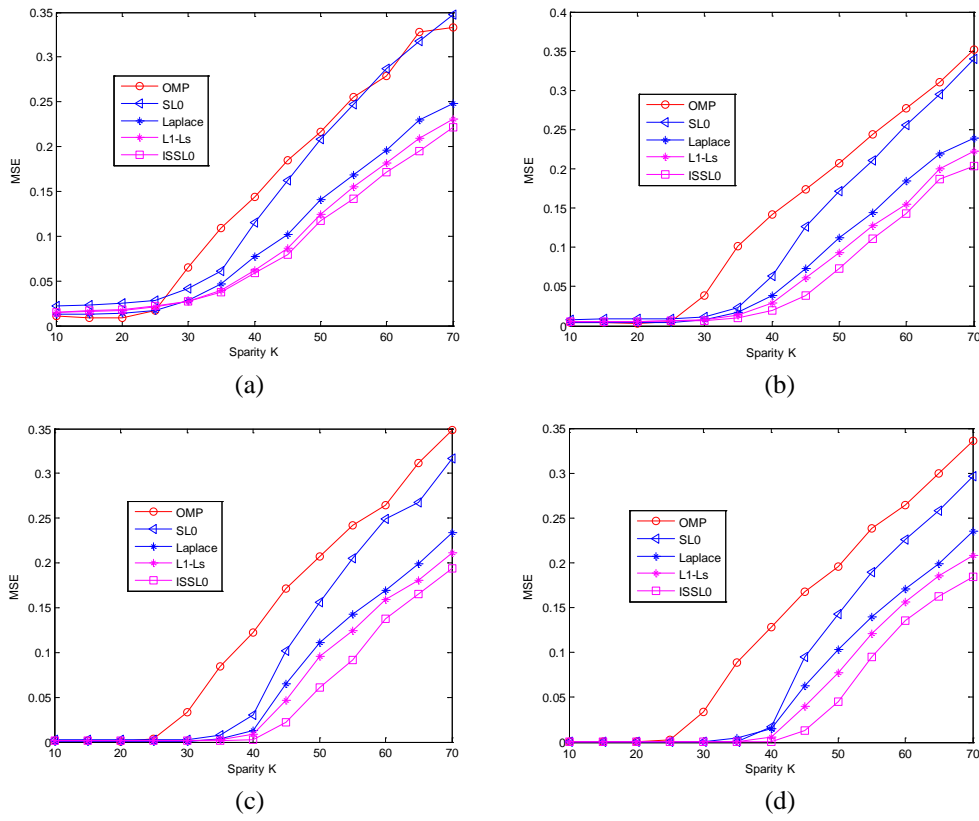
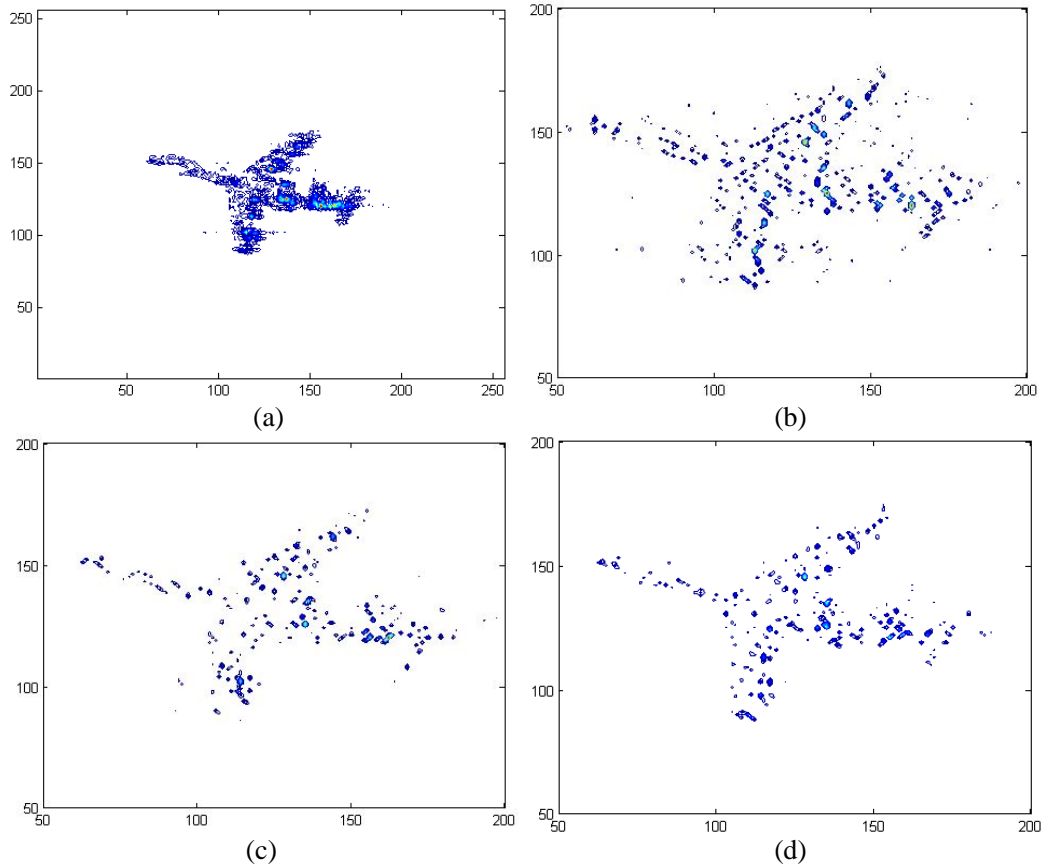


Fig. 3. MSE for different K (a) SNR = 15dB, (b) SNR = 20 dB (c) SNR =25dB, (d) SNR = 30 dB

Simulation 2. ISAR imaging using real data

In this section, a set of real data of the Yak-42 plane is used to demonstrate the performance of the proposed ISAR imaging algorithm. The related parameters descriptions of the radar data are listed as follows: the carrier frequency is 10 GHz with signal bandwidth of 400 MHz, a range resolution is 0.375 m. The pulse repetition frequency is 50 Hz, i.e., 256 pulses are used in this experiment. Two different amounts of pulses (32-snapshot and 64-snapshot) are implemented. The ISAR images are reconstructed with 256 Doppler bins (that means the size of ISAR is 256×256) is shown as **Fig. 4 (a)**. The experimental results are compared visually and quantitatively to those images obtained by some sparse signal recovery methods including OMP, Bayesian method with Laplace prior and SL0 methods. From **Fig. 4 (b), (c), (d), (e), (f)** and **Fig. 5**. It is noticeable that more amount of pulses generally lead to better imagery results. For 32 snapshots case, images using OMP method has many clutter points. Compared with the other four imaging methods, the proposed ISAR imaging framework generates a better visual quality and has competitive performance. We can see that the ISSLO method generates a better visual quality and the ISAR imaging is more intensive. The noticeable advantage of the ISSLO imaging method is that the strong scatterers of the target are extracted well along with fewer false points. The time of 32 snapshots is only one eighth of the original 256 snapshots acquirement time. It is possible to image maneuvering target in a short time duration using sparse signal recovery algorithms.



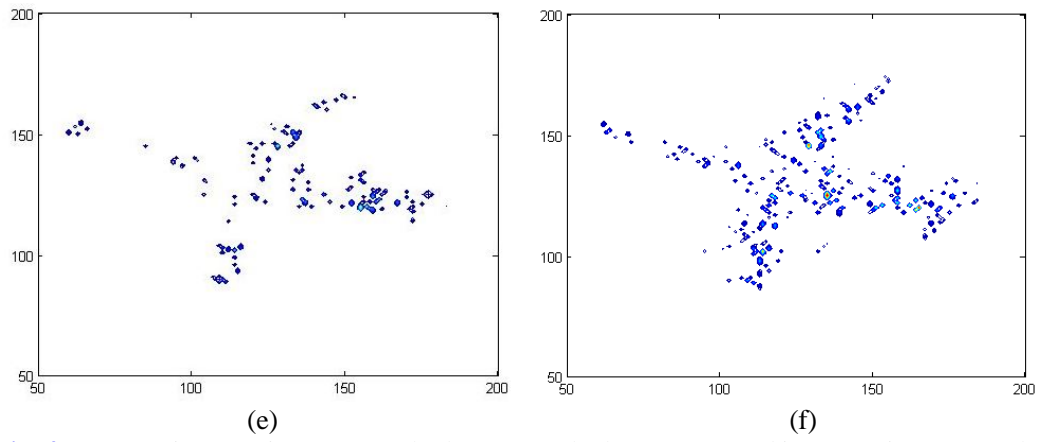
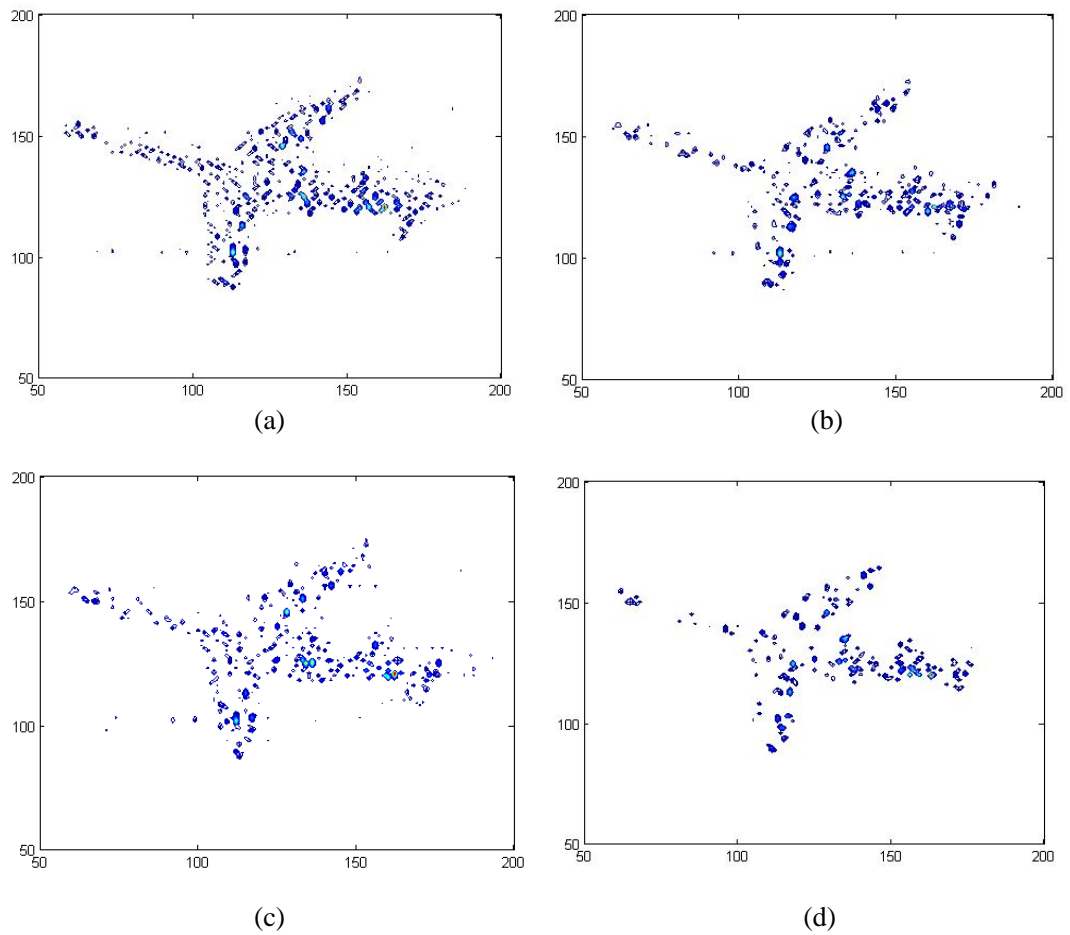


Fig. 4. (a) ISAR image using 256 samples by FFT method, Reconstructed images using 32 snapshots, (b) OMP (c) Bayesian method (d) l1-ls (e) SL0 (f) ISSL0



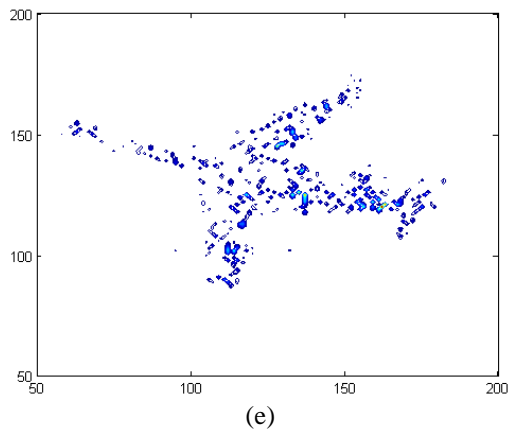


Fig. 5. Reconstructed images using 64 snapshots, (a) OMP (b) Bayesian method (c) l1-ls (d)SL0 (e) ISSLO

5. Conclusion

In this paper, one improved sparse signal recovery algorithm based on SL0 algorithm is demonstrated to improve ISAR imaging with limited pulse numbers. We propose one new continuous function as smoothed function sequence to approximate l_0 norm, then single loop step is used to replace two loop layers in SL0 algorithm to ensure the reconstruction accuracy without increasing computation amounts. Simulation results show that the performance of ISSLO algorithm is superior than OMP, Bayesian method with Laplace prior, l1-ls and SL0 methods. The real data experiments show the proposed algorithm can improve imaging quality.

References

- [1] D. H. Kim, D. K. Seo and H. T. Kim, "Efficient classification of ISAR images," *IEEE Transaction on Antennas and Propagation*, vol. 53, no. 5, pp.1611–1621, May, 2005. [Article \(CrossRef Link\)](#)
- [2] M. Xing, R. Wu, Y. Li and Z. Bao, "New ISAR imaging algorithm based on modified Wigner Ville Distribution," *IET Radar, Sonar and Navigation*, vol. 3, no. 1, pp.70–80, Jan. 2009. [Article \(CrossRef Link\)](#)
- [3] H. Wang, Y. Qun, M. Xing and S. Zhang, "ISAR imaging via sparse probing frequencies," *IEEE Geosci.Remote Sens.Lett.*, vol. 8, no. 3, pp.451–455, May. 2011. [Article \(CrossRef Link\)](#)
- [4] E. Candes, J. Romberg and T. Tao, "Robust uncertainty principles: Exact signal reconstruction from highly incomplete frequency information," *Transactions on Information Theory*, vol. 52, no.2, pp. 489–509, Feb, 2006. [Article \(CrossRef Link\)](#)
- [5] E. J. Candès, M. B.Wakin, "An introduction to compressive sampling," *IEEE Signal Processing Magazine*, vol. 25, no. 2, pp.21–30, Feb, 2008. [Article \(CrossRef Link\)](#)
- [6] B. Demba, B. Behtash and L. P. Patrick, "Convergence and Stability of Iteratively Re-weighted Least Squares Algorithms," *Transaction on Signal Processing*, vol. 62, no. 1, pp.183–195, Jan. 2014. [Article \(CrossRef Link\)](#)
- [7] H.Q. Gao, R.F. Song, "Distributed compressive sensing based channel feedback scheme for massive antenna arrays with spatial correlation," *KSII Transactions on Internet and Information Systems*, vol.8, no.1, pp.108-122, Jan. 2014. [Article \(CrossRef Link\)](#)

- [8] Y.J. Li, R.F. Song, "A new compressive feedback scheme based on distributed compressed sensing for time-correlated mimo channel," *KSII Transactions on Internet and Information Systems*, vol.6, no.2, pp.580-592, Feb. 2012. [Article \(CrossRef Link\)](#)
- [9] H. Anh, I.Koo, "Primary user localization using Bayesian compressive sensing and path-loss exponent estimation for cognitive radio networks," *KSII Transactions on Internet and Information Systems*, vol.7, no.10, pp.2338-2356, Oct. 2013. [Article \(CrossRef Link\)](#)
- [10] R. Chartrand. "Exact reconstruction of sparse signals via nonconvex minimization," *IEEE Signal Processing Letters*, vol. 14, no. 10, pp.707-710, Oct.2007. [Article \(CrossRef Link\)](#)
- [11] J. A. Tropp, A. C. Gilbert, "Signal Recovery from Random Measurements via Orthogonal Matching Pursuit," *IEEE Transactions on Information Theory*, vol. 53,no.12, pp.4655-4666, Dec.2007. [Article \(CrossRef Link\)](#)
- [12] D. Needell, R. Vershynin, "Signal Recovery From Incomplete and Inaccurate Measurements Via Regularized Orthogonal Matching Pursuit," *IEEE Journal of Selected Topics in Signal Processing*, vol. 4, no.2, pp.310-316, April. 2010. [Article \(CrossRef Link\)](#)
- [13] H. Mohimani, M. Babaie-Zadeh, C. Jutten, "A fast approach for overcomplete sparse decomposition based on smoothed ℓ_0 norm," *IEEE Transaction Signal Processing*, vol.57, no.1, pp.289-301, Jan. 2009. [Article \(CrossRef Link\)](#)
- [14] L. C. Potter, E. Ertin, J. T. Parker and M. Cetin, "Sparsity and compressed sensing in radar imaging," in *Proc. of the IEEE*, vol.98, no.6, pp.1006-1020, June. 2010.[Article \(CrossRef Link\)](#)
- [15] M. Tello, P. Lopez-Dekker and J. Mallorqui, "A novel strategy for radar imaging based on compressive sensing," *IEEE Trans. Geosci.Remote Sens.*, vol.48, no.12, pp.4285-4295, Dec. 2010. [Article \(CrossRef Link\)](#)
- [16] X. C. Xie, Y. H. Zhang, "High-resolution imaging of moving train by ground-based radar with compressive sensing," *Electron Letters*, vol.46, no.7, pp.529-531, April, 2010. [Article \(CrossRef Link\)](#)
- [17] M. Cetin, I. Stojanovic, N. Onhon, K. R. Varshney, S. Samadi, W. C. Karl and A. S. Willsky, "Sparsity Driven synthetic aperture radar imaging Reconstruction, autofocusing, moving targets, and compressed sensing," *IEEE Signal Processing Magazine*, vol.31, no.4, pp.27-40, April, 2014. [Article \(CrossRef Link\)](#)
- [18] V. M. Patel, G. R. Easley, D.M. Healy and R. Chellappa, "Compressed synthetic aperture radar," *IEEE Journal of Selected Topics in Signal Processing*, vol. 4, no. 2, pp.244-254, April, 2010. [Article \(CrossRef Link\)](#)
- [19] C. He, L. Z. Liu, L. Y. Xu and M. Liu, "Learning Based Compressed Sensing for SAR Image Super-Resolution," *IEEE Journal of Selected Topics in Applied Earth Observation and Remote Sensing*, vol. 5, no. 4, pp.1272-1281, Aug, 2012. [Article \(CrossRef Link\)](#)
- [20] X. Tan, W. Roberts, J. Li and P. Stoica, "Sparse learning via iterative minimization with application to mimo radar imaging," *IEEE Transactions on Signal Processing*, vol. 59, no.3, pp 1088-1101, March, 2011. [Article \(CrossRef Link\)](#)
- [21] D.Li, W.D. Chen, "MIMO radar Sparse Imaging with phase mismatch," *IEEE Geoscience and Remote Sensing Letters*, vol. 12, no. 11, pp. 816-820, April, 2014. [Article \(CrossRef Link\)](#)
- [22] L. Zhang, M. Xing and C. W. Qiu, "Achieving higher resolution isar imaging with limited pulses Via compressed sampling," *IEEE Geosci. Remote Sens. Lett.*, vol.6, no.3, pp. 567-571, July, 2009. [Article \(CrossRef Link\)](#)
- [23] X. H. Zhang, T. Bai, H. Y. Meng and J. W. Chen, "Compressive Sensing-Based ISAR Imaging via The Combination of the Sparsity and Nonlocal Total Variation," *IEEE Geosci. Remote Sens. Lett.*, vol.11, no.5, pp. 990-994, May, 2014. [Article \(CrossRef Link\)](#)
- [24] R. G. Raj, M. Farshchian, "ISAR imaging in sea clutter via compressive sensing," *International Waveform Diversity and Design Conference (WDD)*, 200-205, Aug, 2010. [Article \(CrossRef Link\)](#)
- [25] L. F. Zhao, L. Wang, G. Bi and L. Yang, "An Autofocus Technique for High-resolution Inverse Synthetic Aperture Radar Imagery," *IEEE Trans. Geosci.Remote Sens.*, vol.52, no.10, pp. 6392-6403, Oct. 2014. [Article \(CrossRef Link\)](#)

- [26] W. Qiu, H. Z. Zhao, J. X. Zhou and Q. Fu, "High-Resolution Fully Polarimetric ISAR Imaging Based on Compressive Sensing," *IEEE Geoscience and Remote Sensing*, vol.52, no.10, pp.6119-6131, Oct. 2014. [Article \(CrossRef Link\)](#)



Junjie Feng received the B.E. and M.S. degrees from the Baoji University of Arts and Science and the Zhongyuan University of Technology in 2006 and 2010, respectively. He is currently pursuing the Ph.D. degree with the Nanjing University of Aeronautics and Astronautics, China. His research interests include radar signal processing and wireless communication.



Gong Zhang received the Ph.D. degree in electronic engineering from the Nanjing University of Aeronautics and Astronautics (NUAA), Nanjing, China, in 2002. From 1990 to 1998, he was a Member of Technical Staff at No724 Institute China Shipbuilding Industry Corporation (CSIC), Nanjing. Since 1998, he has been with the College of Electronic and Information Engineering, NUAA, where he is currently a Professor. His research interests include radar signal processing and classification recognition. Dr. Zhang is a member of Committee of Electromagnetic Information, Chinese Society of Astronautics (CEI-CSA) and a Senior Member of the Chinese Institute of Electronics (CIE).